energies

Article

Smart Hydropower Water Distribution Networks, Use of Artificial Intelligence Methods and Metaheuristic Algorithms to Generate Energy from Existing Water Supply Networks

Diamantis Karakatsanis and Nicolaos Theodossiou *

Division of Hydraulics and Environmental Engineering, Department of Civil Engineering, Aristotle University of Thessaloniki, 541 24 Thessaloniki, Greece; dkarakat@civil.auth.gr
* Correspondence: niktheod@civil.auth.gr

Abstract: In this paper, the possibility of installing small hydraulic turbines in existing water-supply networks, which exploit the daily pressure fluctuations in order to produce energy, is examined. For this purpose, a network of five pressure sensors is developed, which is connected to an artificial intelligence system in order to predict the daily pressure values of all nodes of the network. The sensors are placed at the critical nodes of the network. The locations of the critical nodes are implemented by applying graph theory algorithms to the water distribution network. EPANET software is used to generate the artificial intelligence training data with an appropriate external call from a Python script. Then, an improvement model is implemented using the Harmony Search Algorithm in order to calculate the daily pressure program, which can be allocated to the turbines and, consequently, the maximum energy production. The proposed methodology is applied to a benchmark water supply network and the results are presented.

Keywords: WDNs; harmony search algorithm; machine learning; graph theory; micro hydro generator; wireless sensor network

Citation: Karakatsanis, D.; Theodossiou, N. Smart Hydropower Water Distribution Networks, Use of Artificial Intelligence Methods and Metaheuristic Algorithms to Generate Energy from Existing Water Supply Networks. *Energies* **2022**, *15*, 5166. https://doi.org/10.3390/en15145166

Academic Editors: Helena M. Ramos and Alberto Geri

Received: 11 March 2022
Accepted: 8 July 2022
Published: 16 July 2022

1. Introduction

Water pressure management is one of the main issues in water distribution networks (WDNs) as it is related to water and energy saving [1]. High-pressure values are directly connected to leaks, water losses, and damage of pipes, especially in old WDNs [2]. Given that the hourly water demand changes significantly during 24 h, corresponding changes are created in the pressure of the network nodes. The problem becomes more acute during the hours when water demand is low. There are several papers in the literature on the relationship between pressure and water loss [3–5], as well as strategies and methodologies for reducing pressure using control valves (PRV) [6–8] aiming at leakage reduction through the minimization of the water pressures. Metaheuristic algorithms such as the harmony search algorithm have also been used to optimally set and position pressure reduce valves [9]. This group of algorithms has proven to be very effective in solving nonlinear problems without requiring high computational resources [10–12].

Each node of the network has a minimum pressure requirement, depending on the altitude, the height of the buildings, the losses in the pipes, etc., and when this is satisfied a strategy for managing the extra pressure at the nodes is necessary. The most common solution for pressure management in the literature is to maintain a constant pressure at specific nodes; although, various real-time applications that use monitoring pressure sensor measurements in order to adjust the pressure of the nodes according to demand have been proposed [13,14]. The pressure needs to be set high enough to still satisfy customers' needs subject to a minimum pressure target.

However, a head drop in any PRV is an energy dissipation that could be an opportunity to generate electricity power [15–18]. Power potential recovery from water networks can be implemented in various ways in order to allow both an efficient power conversion and a reliable network pressure regulation [19,20]. A popular methodology is PATs (Pumps As Turbines). The function of a PAT is to convert the kinetic energy and pressure energy of the fluid into mechanical energy of the rotor according to the pressure requirements at the nodes of the downstream network. During the day, when the needs for water and pressure at the nodes are greater than at night, the PAT acts as a pump ensuring the required flow and pressure, especially at the highest nodes of the network. During the evening hours when water needs are lower the PAT can operate as a power turbine exploiting the daily excess water in the tanks. In this case, the PAT should be placed downstream of the tank so that it generates gravity energy at night. In addition to generating electricity, PATs contribute significantly to reducing node pressure and thus minimize water loss and pipeline failure. The most common practice for limiting high pressure is to use pressure relief valves (PRV). Replacing them or operating in parallel with PAT can effectively control pressure even if the power recovery is low. In particular, installing PAT on existing WDNs can be a viable option to reduce the consequences of high pressure without excessive installation costs and if combined with another renewable energy source, can have significant energy benefits [21]. A pump system that works both as a pump and as a turbine can be used as micro-pump storage. In this case, the micro-pump system is connected with water tanks. Operating as a pump, the micro-pump system transports water from low to high potential storing energy, while operating as a turbine, it uses the stored water to generate electricity [22]. The most important advantages of PAT are the simplicity of installation instead of a conventional turbine for this kind of application and the low investment cost. Usually, in WDN, the water supplies range between 0.01 and 0.5 m^3/s and the pressure load between 1 and 100 m. In these ranges, the conventional types of turbines (Pelton, Francis, Kaplan, etc.) can be barely functional [23]. In the literature, the financial analyses show a payback period of the installation cost of a PAT system of about 2 to 3 years; although, the efficiency of PATs is lower than that of conventional systems. [24] In order to evaluate investment proposals in energy recovery systems, cost classification systems have been developed using corresponding cost groups from hydropower plants. [25] In addition, many computational models and methods of financial evaluation have been developed. These models predict the cost of PAT from the nominal water flow and the available hydraulic head [26] or choose PATs whose operating point gives the minimum payback time [27]. As PATs replace or operate in parallel with PRVs, another approach is to choose the most economical solution between PATs and PRVs using the Net Present Value [28].

The idea of using pumps as turbines dates back to the 1930s and studies focus on predicting the operation curve of the turbine from the pump curve. Some of these studies use experimental data for pump reverse operation [29], but most use mathematical models to predict the turbine curve in contrast to costly laboratory experiments. For this purpose, in the literature, there are various methods for predicting the operation curve of the turbines that use artificial neural networks [30,31] or various optimization methods in combination with statistical correlations. Simplified theoretical models as well as physics-based models are also quite common in trying to predict the reverse operation of the pump [32–34]. Most of the malfunctions of PATs are related to the lack of performance data during the reverse hydraulic operation of the pumps by the manufacturers and consequently the need to generate experimental data or to develop models for predicting the turbine performance from the pump data. Most models aim to predict the PAT Best Efficiency Point (BEP) of the PAT by knowing the BEP of the pump from the manufacturer's manuals. However, the use of PATs or the replacement of PRVs by PATs does not constitute an immediate recovery of lost energy and the main reason for this is the difference between the operating curves of pumps and turbines. In other words, a pump with the best possible efficiency may display small efficiencies during a reversal mode. For these reasons the use of PATs in existing WDNs should be implemented in the context of integrated financial planning and feasibility studies, which should prove the viability of the installation. However, there are many case studies of PAT technology on water distribution networks. Table 1 shows some important publications on PAT applications in WDNs.

Table 1. Case studies of energy recovery.

Subject	Case Study Location	Reference
A technical overview of the design and the outcomes of a first-of-its-kind Pumped Hydro Energy Storage (PHES) micro facility	Froyennes, Belgium	Morabito (2019) [35]
Experimental activity to select pumps running as turbines in micro-hydro plants	Cosenza, Italy	Barbarelli (2017) [36]
Energy recovery from replacing PRVs with MHPs in the WDN	Tehran, Iran	Hamlehdar (2022) [37]
Determines the potential of the water supply and effluent treatment system for generating electricity	Pato Branco, Brazil	Da Silva BLA (2011) [38]
Control pressure within a district of Naples water distribution network, showing large potential revenues of PATs	Napoli, Italy	Giugni M. (2009) [39]
Telemetry data from control valves and pressure-reducing valves within the Dublin city water supply network are analyzed to identify suitable locations for energy recovery	Dublin, Ireland	Corcoran L. (2012) [40]
Identifying Hydropower Potential of Alpine Regions	Carinthia, Austria	M. Möderl (2012) [41]
Economic feasibility analysis of substituting existing pressure reduction valves (PRVs) with pumps used as turbines (PaTs) in two real Italian water distribution networks (WDN)	Murgia—Central Apulia, Italy	Balacco (2020) [42]
Proposes an energy sustainability score for benchmarking WDNs	Kolkata, India	Zaman (2021) [43]
influence of the leakages in energy recovery systems at irrigation networks	Vallada. Spain	Carlos Andrés Macías Ávila (2021) [44]
Proposes a framework for WDN by reconfiguring the original network layout into (dynamic) district metered areas	Parete, Italy	Giudicianni (2020) [45]
Real-Time Control of Pressure and Hydropower Generation	Benevento, Italy	Fontana (2018) [46]
Genetic algorithm to optimize the regulation of PAT settings.	Catania, Italy	Creaco (2020) [47]
A hybrid PAT with solar pilot system and a traditional diesel generator in an off-grid farm.	Cordoba, Spain	García (2021) [48]

In the present paper, a combined method of real-time monitoring of the pressure value with methods of artificial intelligence and metaheuristic optimization methods is proposed, which searches for time opportunity "windows" of electricity production during the operation of the water supply network in real time. The hierarchical flow diagram of the methodology proposed in the present work is presented in Figure 1. The novel proposed methodology looks for power generation opportunities from WDNs during their operation. The three main issues analyzed in the methodology are: at which nodes the PATs will be placed, at which time steps they will be activated within 24 h, and how much theoretical energy is available for recovery without creating problems in the operation of the network. In the literature, similar strategies for real-time management of energy production using AAN have been proposed [49]. The innovation elements of the proposed method are: the combined use of an artificial intelligence method with a metaheuristic algorithm at the same model and an attempt to answer the three questions mentioned above: PAT position, activation time, and how much pressure to exploit.

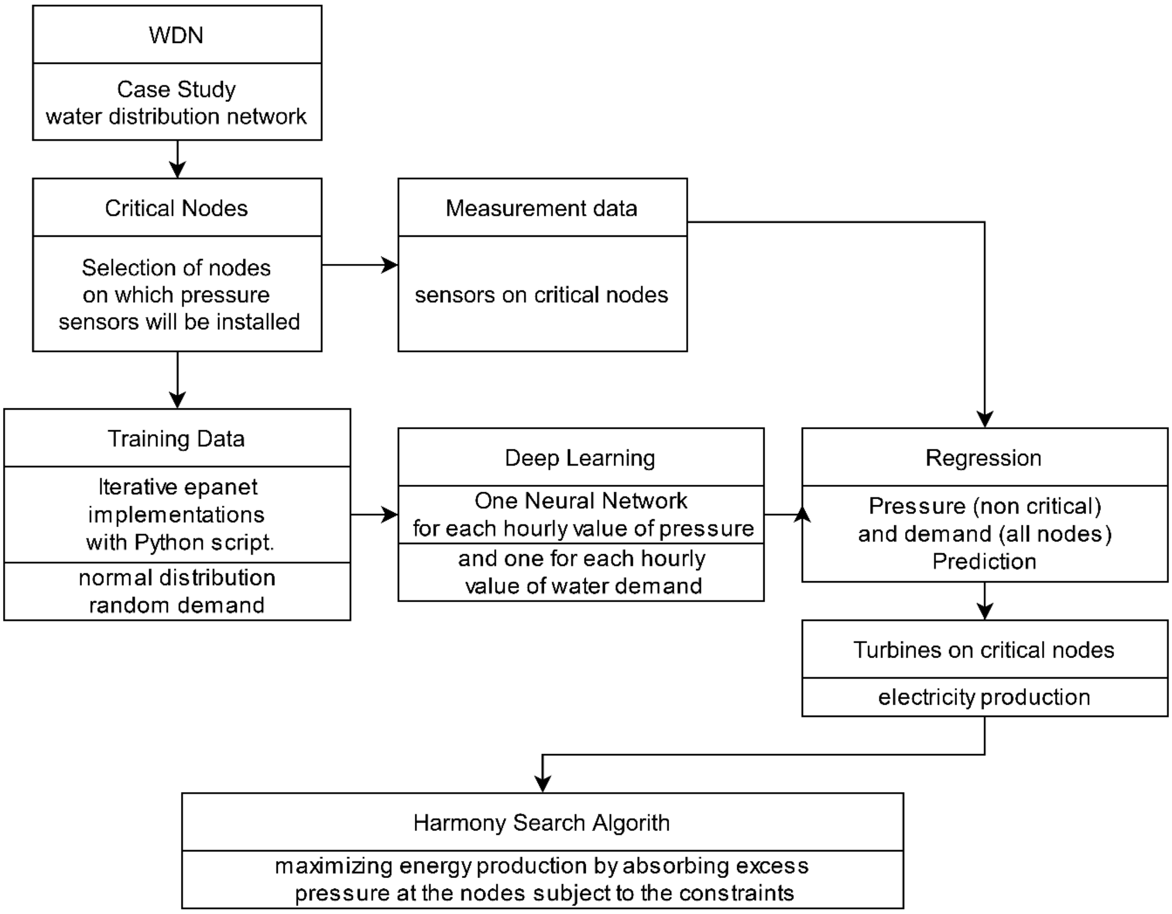

Figure 1. Hierarchical flow diagram of the methodology.

2. Benchmark Water Distribution Network

The proposed methodology in this paper will be applied to the WDN studied by Jowitt and Xu [50], which is reproduced in Figure 2. This network is a benchmark Water Distribution System, which is very often used to verify optimization methods in water supply networks such as optimal valve location in [51–53] and PAT localization problems in [54]. The network consists of 37 links, 22 nodes, and 3 reservoirs. The characteristics of each link are given in Table 2, and the elevation of each node in Figure 2. The minimum pressure for each node is set at 20 m and the Hazen Williams formula is used to calculate the friction losses. In the literature, the water demand is usually taken as an hourly average with the highest peaks at noon. Given the hourly demand, the average daily is also obtained. From the average daily demand is calculated the maximum daily usually with some peak rates [55], which depend on the population that serves the network. However, the most critical parameter for the failure of a water supply network is the instantaneous demand [56]. That is, the percentage of the population that will use water at the same time. Various methods have been proposed for instantaneous demand calculation, but the stochastic generators are considered to approach the real value in a more rational way. The water demand at the nodes is a parameter that will be predicted by the neural networks based on the pressure at specific nodes. Therefore, for the training of neural networks, it is necessary to create a set of data on hourly water demand. For all the above reasons, the random normal distribution with a base value of 5 L/s is chosen, which is described in Equation (1).

$$p(x) = \frac{1}{\sqrt{2\pi\sigma^2}} e^{-\frac{(x-\mu)^2}{2\sigma^2}} \tag{1}$$

where μ = 1 is the mean and σ =2 is the standard deviation.

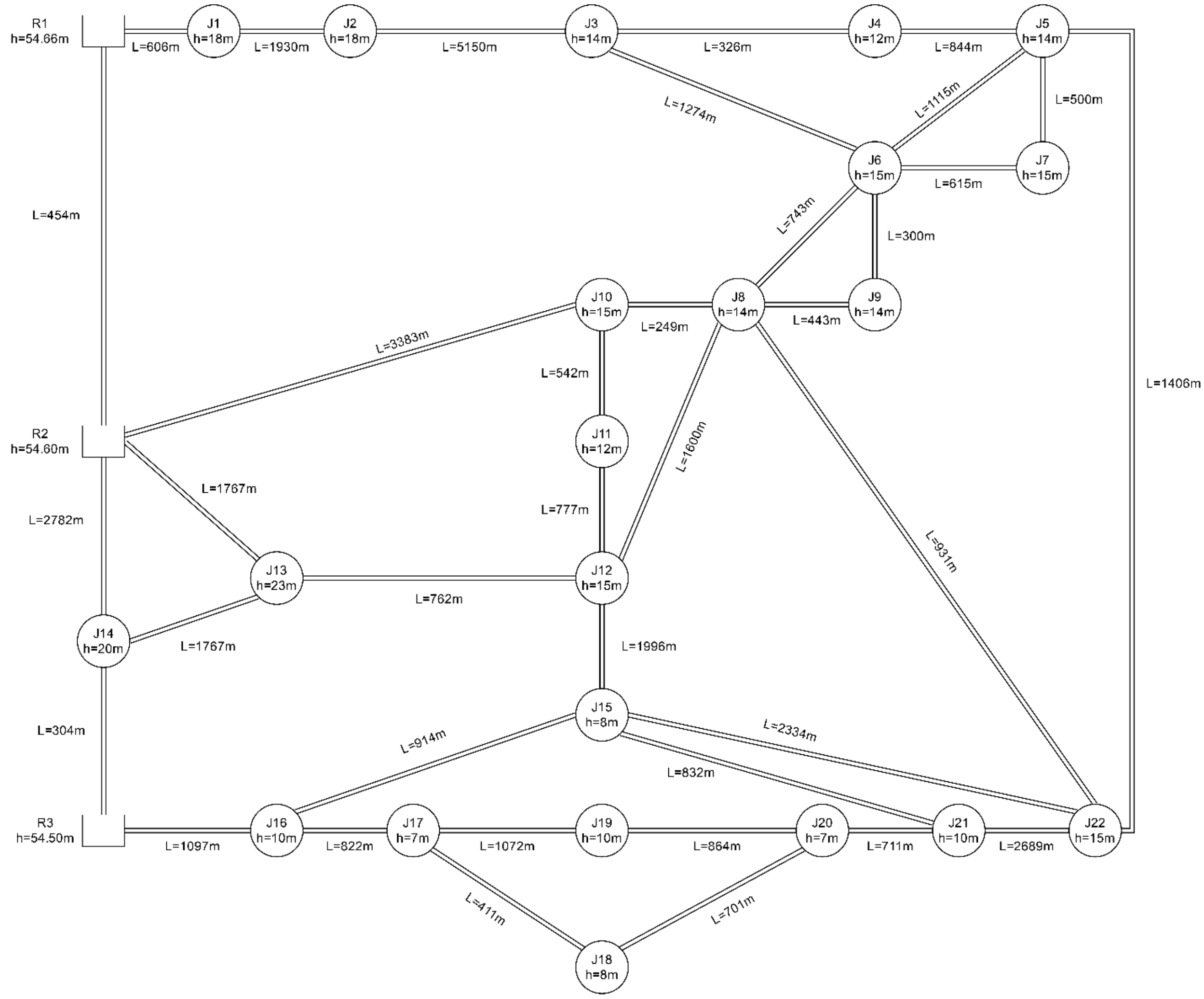

Figure 2. Sketch diagram of Jowitt and Xu Water Distribution System.

Table 2. Link IDs, Diameters, and Lengths of the WDN under investigation.

Link ID	Diameter (mm)	Length (m)	Link ID	Diameter (mm)	Length (m)	Link ID	Diameter (mm)	Length (m)
Pipe P1	457	606	*Pipe P13*	305	249	*Pipe P25*	381	1097
Pipe P2	457	1930	*Pipe P14*	305	3383	*Pipe P26*	229	914
Pipe P3	305	5150	*Pipe P15*	152	1406	*Pipe P27*	152	832
Pipe P4	152	326	*Pipe P16*	229	931	*Pipe P28*	305	822
Pipe P5	229	844	*Pipe P17*	152	2334	*Pipe P29*	229	1072
Pipe P6	381	500	*Pipe P18*	457	1600	*Pipe P30*	152	864
Pipe P7	152	1274	*Pipe P19*	457	762	*Pipe P31*	152	411
Pipe P8	229	1115	*Pipe P20*	475	1767	*Pipe P32*	152	711
Pipe P9	381	615	*Pipe P21*	381	1014	*Pipe P33*	152	2689
Pipe P10	229	300	*Pipe P22*	457	454	*Pipe P34*	229	542
Pipe P11	381	743	*Pipe P23*	229	2782	*Pipe P35*	229	1996
Pipe P12	229	443	*Pipe P24*	381	304	*Pipe P36*	229	777
						Pipe P37	229	701

This ensures training of the neural network in several combinations of instantaneous water demand and therefore a better response to the demand forecast from the pressure values at the critical nodes.

3. Critical Nodes

In order to monitor the pressure values in real time, it is necessary to install a network of sensors (WSN). Each sensor should have a wireless communication system with a sink node, which is then connected to a gateway that can collect data from various networks. The gateway transfers data to a data center where they are stored, processed, analyzed, and received by the user. A typical WSN is shown in Figure 3. A real-time WSN to be effective, all the necessary computing processes must be performed in the shortest possible computing time. This is not always possible when complex and time-consuming calculations are required.

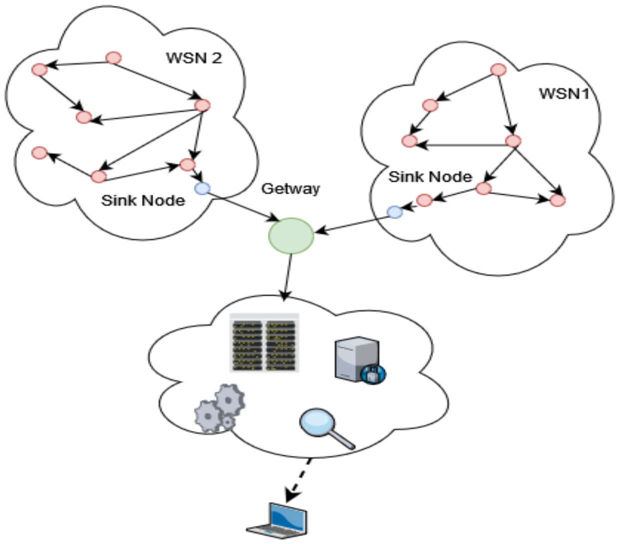

Figure 3. Typical WSN structure.

An ideal situation for monitoring node pressures in real time would be to install sensors at each network junction. This is not economically acceptable due mainly to the high cost of the initial installation of the network, so a strategy should be sought that will select the least possible and most representative nodes for the installation of sensors. A strategy for finding the critical nodes of a WDN is to consider the network as a connected G (V, E) graph where V is the set of nodes and E is the set of links. According to graph theory, the most reliable graph structure is considered to be where each node has the same number of connected edges (pipes). However, in real water-supply networks, especially when new sections are added, the grid may have a random structure. Two graph theory functions are used to select the pressure sensor mounting nodes: closeness centrality and betweenness centrality. Closeness centrality indicates how close a node is to all other nodes in the network. It is calculated as the average of the shortest path length from the node to every other node in the network by Equation (2). The betweenness centrality captures how much a given node u is in-between others. This metric is measured with the number of shortest paths between any couple of nodes in the graphs that pass through the target node u. It is calculated by Equation (3) [57].

$$C(u) = \frac{n-1}{\sum_{u=1}^{n-1} d(v,u)} \tag{2}$$

where d (v,u) is the shortest-path distance between v and u, and n is the number of nodes in the graph.

$$Cb(u) = \sum_{s,t\ E\ V} \frac{\sigma(s,t|u)}{\sigma(s,t)} \tag{3}$$

where V is the set of nodes, $\sigma(s, t)$ is the number of shortest (s, t)-paths, and $\sigma(s, t\,|\,v)$ is the number of those paths passing through some node u other than s, t.

The results from the application of the two functions in the network are presented in Figure 4.

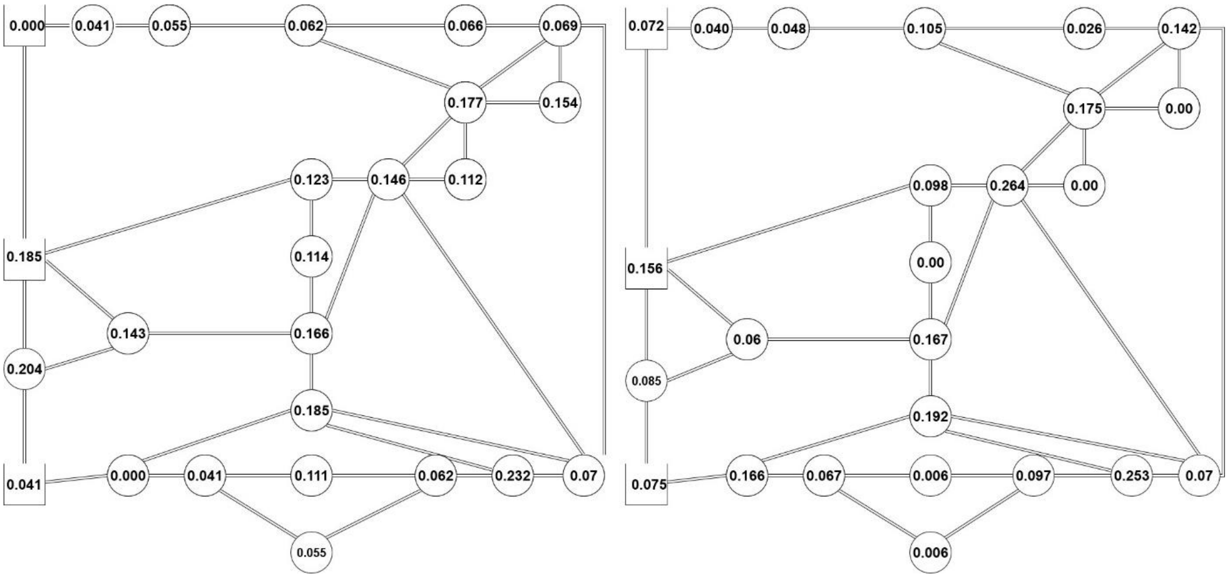

Figure 4. Closeness centrality (**left**) and betweenness centrality (**right**).

The process is organized by the NetworkX [58] python library. It is selected to predict the WDN pressures from 20% of the nodes, i.e., for five nodes. This procedure implements by following three rules based on graph theory functions response.

- Two nodes are selected with the minimum absolute difference between the closeness centrality and the betweenness centrality of the nodes. These nodes are 1 and 12. This rule represents a similar response on both graph theory functions.
- Two next nodes are selected with the maximum absolute difference between the closeness centrality and the betweenness centrality of the nodes and small values for the betweenness centrality. These nodes are 7 and 14. This rule represents the domination of closeness centrality
- The last node is a random selection. This rule introduces randomness in the way that nodes are selected, which is necessary if the methodology is applied to existing WDNs. In this case, it is possible that PATs are already installed on a node that does not comply with the two previous rules.

Finally, nodes 1, 7, 12, 14, 20 are selected.

4. Training Data

For the five nodes selected in the previous chapter, an artificial intelligence system will be organized in order to calculate the hourly pressure values of the other nodes as well as the hourly water demand of all nodes of the network. Ideally, real measurements could be used to train neural networks. As this is not yet available, artificial data will be generated by iteration calls of the Epanet software. The Python WNTR [59] library is used for this purpose after being adapted to the needs of this methodology. The procedure is described in Figure 5.

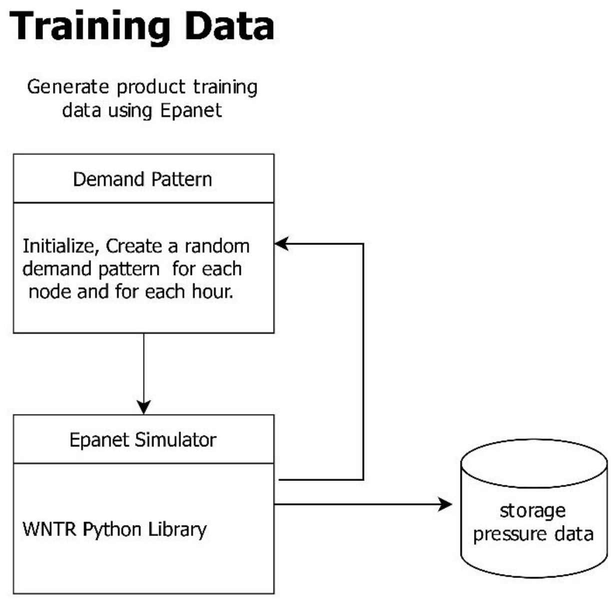

Figure 5. Flowchart of training data procedure.

From the dataset, we will be training a deep learning regression model with columns of input variables (pressure on critical nodes) and output variables (pressure on other nodes and water demand on all nodes). The dataset will be divided into three sections, 70% will be used for training, 15% for validation, and 15% for testing. The pressure data for the 5th and 14th hours are presented in Figure 6.

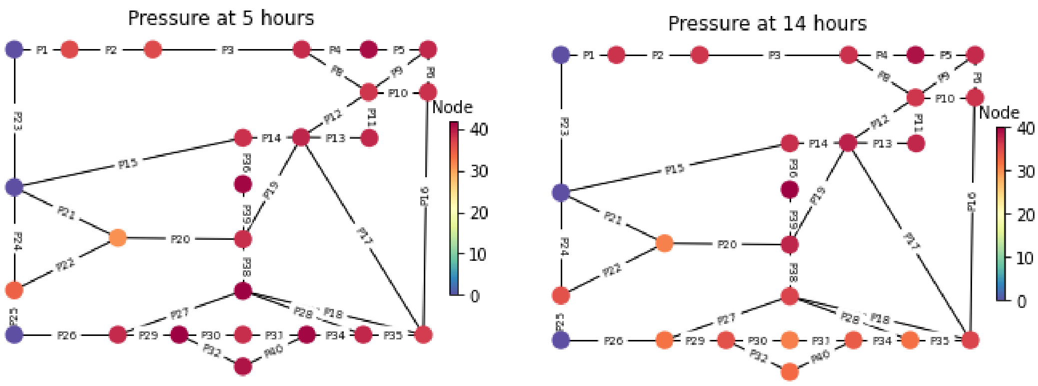

Figure 6. Pressure data for the 5 am and 2 pm.

5. Artificial Neural Networks

The artificial neural network (ANN) is one of the most common ML algorithms. Each artificial neuron is a mathematical nonlinear function, which performs a weighted sum of one or more inputs, which is then passed through an activation function. In the present study, a system of 24 parallel neural networks is created, one for each time step. The aim is to predict the pressure for the nodes that do not have a sensor. For this purpose, these networks will have as input layer 5 vectors of 10,000 values corresponding to a time step (one hour). The output layer consists of 17 vectors of 10,000 values and ReLU is selected as the ANN activation function. The network architecture includes five hidden levels and is shown in Figure 7.

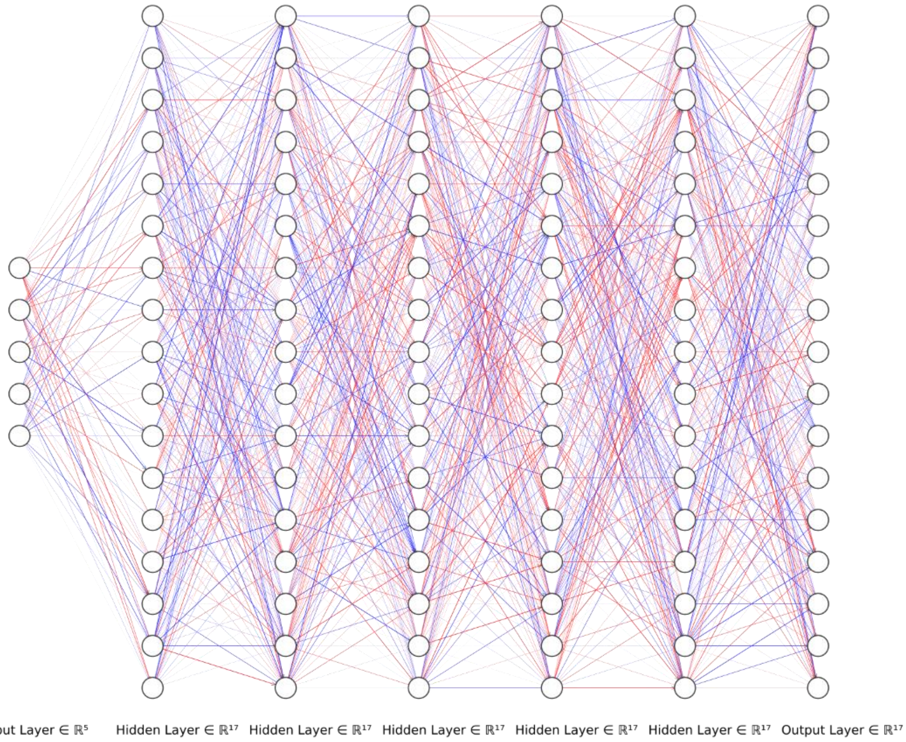

Figure 7. ANN predicts pressure values of non-critical nodes.

The 24 parallel neural networks predict the pressures on the nodes that have no sensors installed. Thus, this system predicts the daily distribution of pressure in the network, and given the Hazen–Williams linear loss formula, since the lengths and diameters of the water pipes are known we can calculate the water flow in each pipe and consequently from the mass balance equation the water demand at each node. This is necessary because in the next step of the process the network will be calculated in a loop of the optimization algorithm in order to maximize energy production. The simulation for the regression model is implemented in the MatLab toolbox and the results for each system are shown in Figure 8.

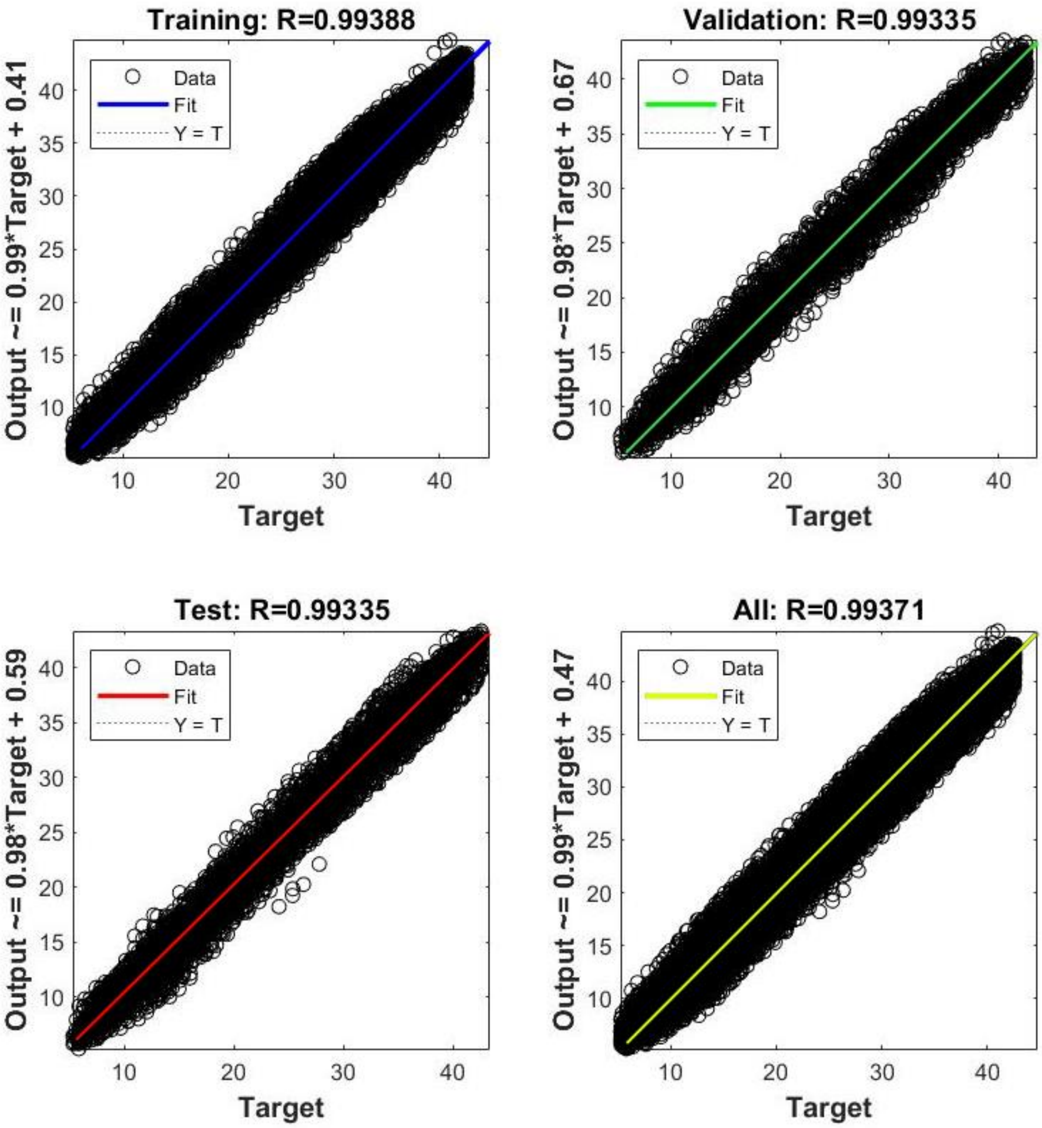

Figure 8. Back propagation neural network R at time step 0.

6. Energy Production

During the evening hours, the water demand decreases resulting in increased pressure at the network nodes. Since the pressure inside the network and at the consumers cannot exceed certain limits, there has to be an excess of pressure in the networks to recover. Increasing the pressure causes damage to the pipes as well as increases water leakage. For this reason, break pressure tanks (BPT) or pressure reduce valves (PRV) are installed at critical points in the network in order to waste pressure excess [60,61]. In the present approach, it is proposed to install turbines at critical node locations, which will recover the dynamic energy when the pressure forecasting system decides that this is possible. This approach proposes the installation of turbines at critical node locations, which will recover the dynamic energy when the pressure forecasting system decides that this is possible. The forecasting system is connected in real time to the sensors so that in live connection, the possibility of excess pressure at any time is predictable. The turbines can be installed in existing networks with the bypass system using PRVs. In order to work in real time, the methodology of the present work must be connected wirelessly to the PRVs of the by-pass system. The addition of by-pass piping changes the hydraulic flow conditions and consequently changes the characteristic operating curve of the PAT. As mentioned in the introduction, a significant disadvantage of PATs is the different operating curve between pump and turbine. The operating curve of the turbine is unknown, as the manufacturers provide information only about the pump. The lack of operating curve data for the turbine mode makes the use of experimental or computational methods necessary to predict the degree of efficiency with specific attention to the off-design operating conditions. For these purposes, combinational models of computational fluid dynamics with experimental tests are developed. In this way, the model is able to predict the performance of PAT with a small error [62,63]. Based on the assumption that the Best Efficiency Point (BEP) of turbine mode is the same as that achieved in pump mode, formulas that evaluate the flow rate and the head exploited by the PaTs have been developed [64,65]. An important tool of recent research is computational fluid dynamics to investigate the internal flow and turbine performance as most studies focus on operation at a constant angular velocity, while there is a need to calculate the performance of the system in conditions of variable rotation [66]. Changes in flow conditions play an important role in the performance of PATs systems, as pump function is more sensitive at the high-pressure side in the spanwise direction than the turbine mode. A comprehensive approach includes CFD simulations and verification of results through experimental data. The simulations include constant flow and rotation conditions as well as variable ones; they can also include different types of pumps [67]. A more multidisciplinary analysis must also take into account the geometric characteristics of the machine. Thus, multi-objective optimization algorithms have been developed, which look for groups of optimal solutions (Pareto Front), replacing the one single optimal answer [68,69]. In addition, CFD simulations are necessary when investigating the effect on the efficiency of specific hydraulic phenomena. For example, the cutwater effect generates local flaws in the flow field, which limit the machine performance or slip phenomenon, which creates deviation of the fluid flow. Computational models that take into account such phenomena allow the identification of the best geometric and hydraulic characteristics of PAT, making its implementation in the field realistic [70,71]. The proposed method concerns the preliminary estimation of the PAT installation, as well as the actual activation time in relation to the daily variability of the pressures through a system of pressure sensors. For this reason, a hypothetical water distribution network has been used without further consideration of PAT performance. In this way, after completing the optimization algorithm, which is presented in the next chapter, using a suitable real-time controller, the pressure percentage of the node that is directed to the turbine is adjusted. The installation is shown schematically in Figure 9. The theoretical power potential of the source is calculated as a function of the hydraulic head and the flowrate by Equation (4).

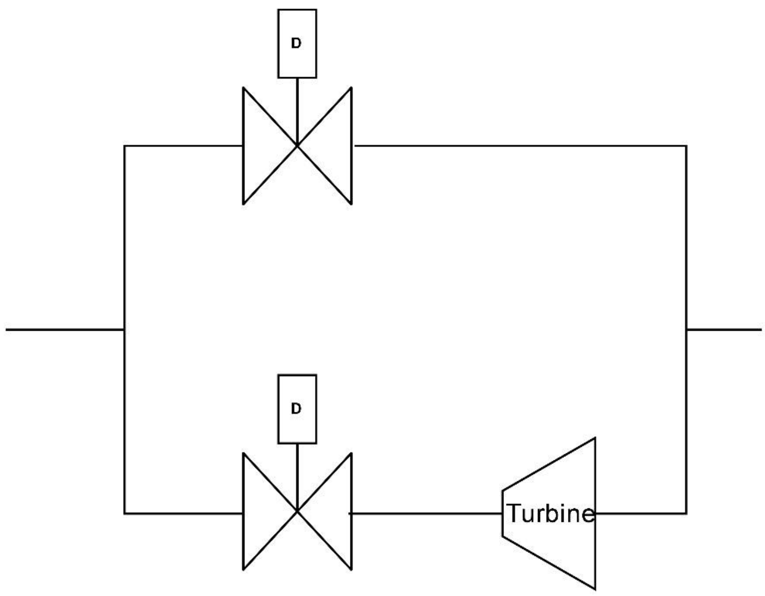

Figure 9. Schematic representation of turbine planting in a water supply network.

$$E_{turbine} = \rho * g * H * Q_{turbine} \quad (4)$$

$E_{turbine}$: The potential power
ρ:The density of water
g: The acceleration of gravity
H: The water head
$Q_{turbine}$: The flowrate across the turbine

7. Optimization Model

Finally, an optimization model is developed using the harmony search algorithm. In order to simulate the above system, the turbine is replaced by a PBV. The network is properly configured and a PRV is placed at each critical node. The network is shown in Figure 10. The optimization model has as variables x1, x2, x3, x4, and x5, which correspond to the percentage of pressure that can be removed from the network per step in order to generate electricity, i.e., the model has 24 × 5 120 variables. The objective function is defined as the sum of the variables and its maximization is requested. The constraints of the model are the minimum pressure on the network nodes in order for the network to serve the consumers. Therefore, for each node, a minimum value of pressure is defined. constrains should also be placed on the maximum pressure in the pipes to prevent damage and water leaks.

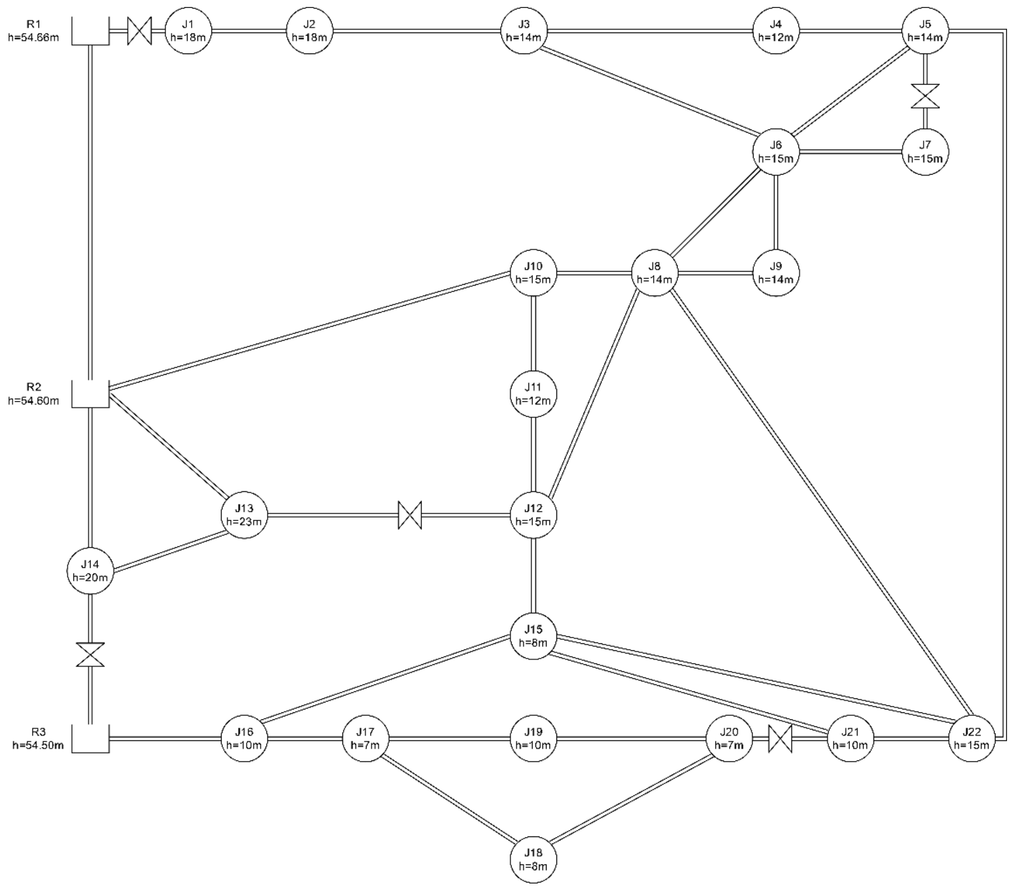

Figure 10. Network with PBV to simulate micro hydropower.

The optimization model is presented in Table 3.

Table 3. The optimization model.

Variables	Constrains	Objective Function
$\overrightarrow{H}_{turbine} = \begin{cases} x1 \\ x2 \\ x3 \\ .. \\ .. \\ x119 \\ x120 \end{cases}$	$P_{min} < P_i < P_{max}$	$F = \sum_{i=1}^{120} x_i$

To calculate the maximum possible pressure that can be removed from the network, the harmony search algorithm is used in combination with the python WNTR library.

8. Harmony Search Algorithm

The Harmony Search Algorithm is a stochastic meta-heuristic method based on the sequential production of possible solutions. It belongs to the category of "neighborhood meta-heuristics" that produces one possible solution (called "harmony") in each iteration. Every possible solution consists of a set of values of the decision variables of the function that needs to be optimized. During the optimization process, a number of "harmonies" equal to the "Harmony Memory Size" are stored in the "Harmony Memory" (HM), a database that includes the produced set of solutions. The optimization process is completed as soon as the predefined total number of iterations has been achieved [72]. Following the definition of the decision variables, the Harmony Memory matrix is formulated. Harmony Memory is m×n matrix, where m is the Harmony Memory Size and n, the number of decision variables included in the objective function. Then, the algorithm begins producing and evaluating new "Harmonies" through the application of HSA's basic mechanisms:

1. Harmony Memory Consideration uses variables' values already stored in the Harmony Memory. This mechanism ensures that good solutions located during the optimization process will contribute to the formation of even better solutions.
2. Some of the solutions selected by the Harmony Memory Consideration mechanism will be slightly altered. This is the second mechanism of the algorithm, named Pitch Adjustment, and it is performed by selecting neighboring values of the decision variables
3. The third mechanism is Improvisation, which introduces new, random elements to the solutions. The probability of introducing such random values is (100-HMCR)%. In this way, the variability of solutions is enriched.

After the creation of a new "Harmony", its performance is evaluated according to the corresponding value of the objective function. If this performance is better than that of the worst "Harmony" stored in the Harmony Memory, it replaces it. This procedure is repeated until the ending criterion is reached.

For the application of the harmony search algorithm, the parameters of the method were given the following values: HMCR = 0.7, PAR = 0.5, and HMS = 10.

The flowchart of the algorithm is shown in Figure 11.

The code is implemented in Python language. A small section appears in Figure 12.

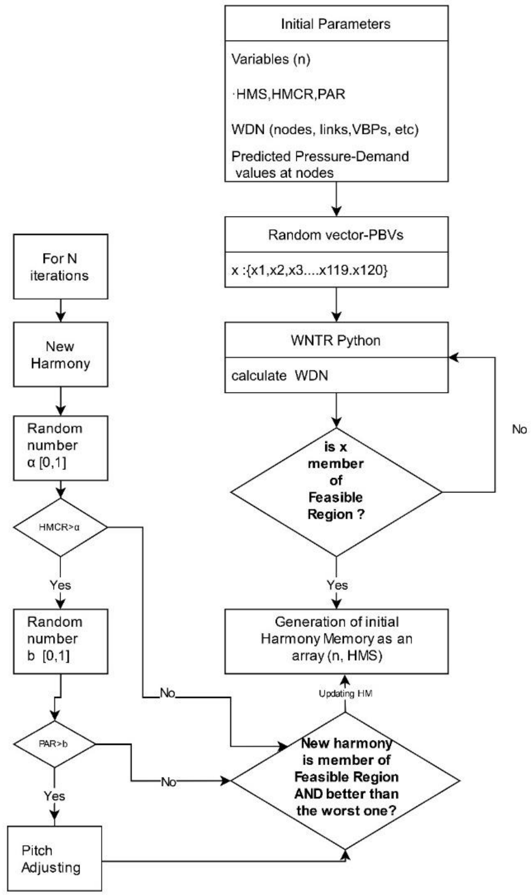

Figure 11. Flowchart of Harmony Search Algorithm.

```
hm = np.array([])
while i < hms+1:
    newharmony = (np.array([random.uniform(1, 20) for i in range(5)]))
    wn.add_valve("v1", "J23", "J1", diameter=0.457, valve_type='PBV', minor_loss=0.0, initial_setting=newharmony[0], initial_status='ACTIVE')
    wn.add_valve("v2", "J24", "J7", diameter=0.381, valve_type='PBV', minor_loss=0.0, initial_setting=newharmony[1], initial_status='ACTIVE')
    wn.add_valve("v3", "J25", "J12", diameter=0.457, valve_type='PBV', minor_loss=0.0, initial_setting=newharmony[2], initial_status='ACTIVE')
    wn.add_valve("v4", "J26", "J14", diameter=0.381, valve_type='PBV', minor_loss=0.0, initial_setting=newharmony[3], initial_status='ACTIVE')
    wn.add_valve("v5", "J27", "J20", diameter=0.152, valve_type='PBV', minor_loss=0.0, initial_setting=newharmony[4], initial_status='ACTIVE')
    sim = wntr.sim.EpanetSimulator(wn)
    results = sim.run_sim()
    pressure_at_1hr = (results.node['pressure'].loc[1*3600, :]).to_numpy()
    if (np.amin(pressure_at_1hr[0:21]))>20 :
        hm=np.append(hm,newharmony)
        i+=1
hm=np.reshape(hm,(5,10))
row= []
for j in range(hms):
    row.append(objective_function(hm[:,j]))
hm=np.vstack([hm,row])

# sorting harmony memory
hmsort = hm[:, hm[-1, :].argsort()]
hmcr= 0.7
par = 0.5
for h in range(1000):
    NewHarmony1=np.array([])
    if random.random()<hmcr:
        for i in range(0,5):
            a=randint(0, hms-1)
            NewHarmony1=np.append(NewHarmony1,hm[i,a])

        if random.random() < par:
            NewHarmony1 = NewHarmony1+random.uniform(-1, 1)
    else:
        NewHarmony1 = (np.array([random.uniform(1, 20) for i in range(5)]))
    wn.reset_initial_values()
```

Figure 12. Source Code of Python Script.

9. Results

The whole process is performed for each time step, i.e., for each hour of the 24 h, and the results for the excess pressure that can be exploited for the energy production are presented in Tables 4 and 5.

Table 4. Excessive pressure at the first 12 h.

Node/Available Pressure (m)	1	2	3	4	5	6	7	8	9	10	11	12
1	12.94	18.14	16.98	9.22	17.20	14.24	15.20	12.37	18.75	11.48	5.94	15.67
7	17.16	5.26	16.92	10.23	16.94	10.12	10.20	11.98	11.79	7.19	6.90	11.98
12	8.18	13.67	12.36	14.73	14.42	13.79	16.13	14.65	14.48	5.60	10.63	12.01
14	16.88	9.44	6.68	16.25	6.97	11.76	9.08	12.71	19.29	17.67	18.48	4.76
20	6.96	17.04	16.35	14.41	14.97	8.67	6.64	15.89	12.41	10.73	16.20	8.84
Sum	62.11	63.55	69.29	64.84	70.50	58.57	57.25	67.61	76.72	52.66	58.14	53.26

Table 5. Excessive pressure at the last 12 h.

Node/Available Pressure (m)	13	14	15	16	17	18	19	20	21	22	23	24
1	17.23	15.46	16.23	1.13	18.23	6.53	17.80	10.25	13.16	13.95	9.61	16.56
7	15.75	19.05	12.35	17.90	7.57	19.18	17.01	13.52	14.59	13.87	17.33	12.61
12	13.26	18.48	9.89	18.33	8.23	16.39	2.11	5.14	14.97	18.19	11.39	14.87
14	5.47	4.72	12.14	9.25	18.19	17.95	17.05	16.62	17.06	10.97	18.12	15.57
20	14.00	18.85	10.75	15.87	17.77	2.03	2.62	12.72	8.10	12.85	8.39	7.98
Sum	65.71	76.57	61.36	62.47	69.98	62.08	56.59	58.24	67.88	69.83	64.83	67.59

Excess pressure can be converted to energy by installing PAT on each selected node (1, 7, 12, 14, and 20) as long as the harmony search algorithm has ensured that the pressure removal from nodes (Tables 4 and 5) will not cause the water supply network to collapse. Each candidate solution vector, as shown in the optimization model (Table 3) ensures a minimum demand pressure for each network node. In this way, we can remove all the excess pressure at any time. The excess pressure and, therefore, the energy produced change significantly during the 24th, depending on the water demand at the nodes of the network. Therefore, the success of the method requires a real-time adjustment of the PATs using a controller that will determine the percentage of the pressure of the node to produce energy based on the result of the optimization model. The aim of this paper is to propose a real-time methodology for exploiting the excess pressure of WDNs. A famous benchmark water network was used for the applicability of the method and, therefore, the results of Tables 4 and 5 also refer to the benchmark test WDN. Nevertheless, the results confirm the success of the method as it discovers excess pressure capable of producing energy in real time and confirm the applicability of the method, by describing all the steps in Figure 1. Based on Equation (4), we can calculate the potential power. Figure 13 shows the theoretical power that can be generated by the PATs for each critical node as well as the total power during the 24th. The diagram shows that theoretical power can be generated with a maximum hourly peak of 9 kW, while the minimum value is 3.8 kW. Of course, in order for the power to be exploitable, the pressure consumed by the PATs in real time must be adjusted, because, as shown in Figure 13, there is a significant variation in the power produced. In any case, those potential power data refer to the benchmark network in order to validate the methodology. Figure 14 shows a whisker power-producing chart for each critical node of the network.

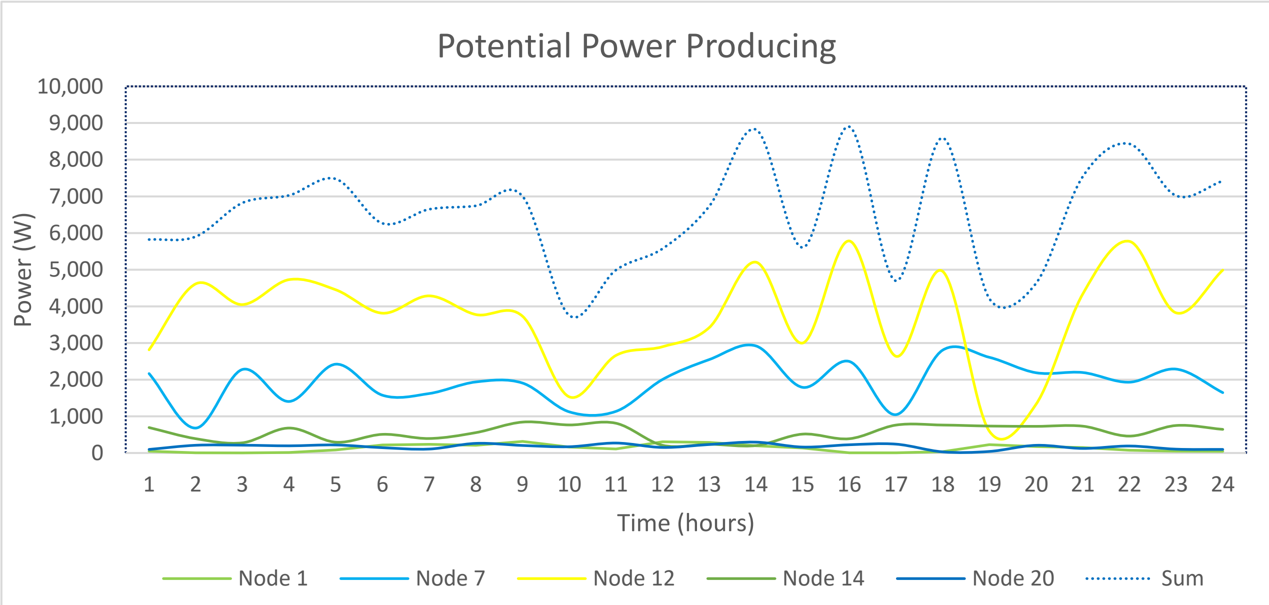

Figure 13. Potential power producing during 24 h.

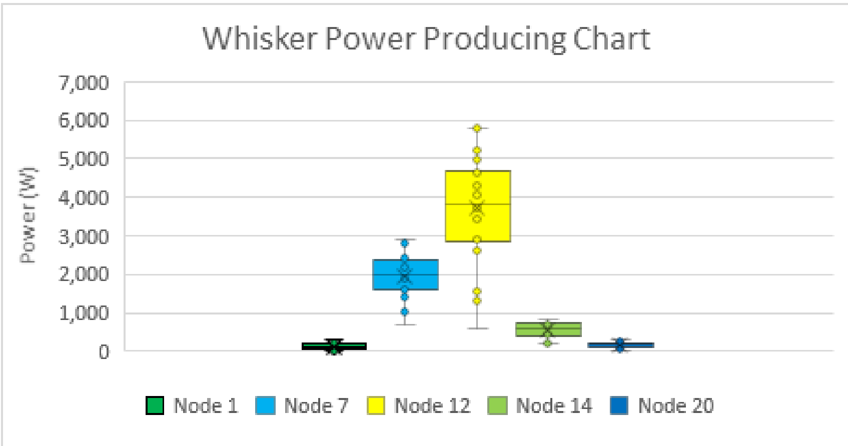

Figure 14. Whisker power producing chart for each critical node.

Figures 13 and 14 show that the contribution of node 12 to energy production is significant but has a huge hourly deviation from the median. Something similar is observed in node 7. On the contrary, nodes 1, 14, and 20 have a small but stable contribution to power generation. This conclusion must be taken into account in the way that the energy produced will be used. This could be a weak point of the method in case we want stable energy production, i.e., in the case that the network directly supplies an energy consumption system such as a street lighting network. In order to make the best use of high energy production peaks, we may need to store the energy produced.

Another important consideration when evaluating the method is the reasonable computational time required to select the percentage of pressure removed from each node. Since the problem is considered to be of high computational complexity and the algorithm should respond in real time, during the simulations the method responded within a reasonable time.

As implied by the simulation results, there is a possibility of generating electricity from existing water supply networks even during peak hours of water demand. In order to apply the method to real networks, a large volume of data is required, so that the artificial intelligence can correctly predict the pressures of the nodes and the water demand. In any case, the installation of mini hydroelectric power plants has increased in recent years in an effort to save energy. In Switzerland, for example, there are 90 small hydropower plants installed in the water supply system. Similar facilities exist in Italy and Austria. Therefore, such a methodology as the one described in the previous chapters could make a significant contribution to energy policy by recovering energy from existing infrastructure projects.

10. Conclusions—Discussion

The proposal of this work is a computational methodology that combines artificial neural networks and metaheuristic algorithms of optimization to apply to a theoretical water distribution network. The algorithm aims to create a sub-network of pressure sensors consisting of 25% of the total nodes of the original network, which is able to predict, using neural networks, the daily changes in the pressures of the rest of the network in real time and without overfitting as presented in Section 5. Properly predicting the pressure from a small subnet of sensors makes the future application of the method economically attractive, as no sensors are required at each node of the original network. Additionally, artificial intelligence drastically reduces network hydraulic computing time, as most calculations are performed during the learning process. In this way, real-time operation of the algorithm is also possible, provided that the subnet sensors are connected wirelessly and the exchange data with a central server. During the future installation of the system on an existing water network after the critical nodes are selected according to Section 3, a reasonable period of training of the algorithm is required, which depends on the number of nodes, but also on the variability of the conditions. In the present work, 10,000 daily values were used, which corresponds to approximately 417 training days. A second network of sensors can be used to confirm the values during the training time, which will be withdrawn after the completion of the process. Alternatively, EPANET software (https://www.epa.gov/water-research/epanet) can be used to calculate unknown pressure values by correcting and training the neural network. This last practice was also used in the present work. After completing the training (either with a second network or EPANET), the algorithm will be able to predict all the pressures in a minimum computational time, which is a critical part of the methodology. Training time can be significantly longer in multi-node networks, but in the process of ANN training data can be shared with another procedure in combination or not with micro-electric power generation. For example, the method could be combined with a leak detection process on WDNs [73]. PATs are placed at critical node locations with a by-pass layout. The aim of this methodology is for the operation of PATs to be possible in all possible opportunities and not only during the hours when the network pressures are high. This is the main question that the proposed methodology tries to answer, if it is possible to activate the power generation system even for a while if there is an opportunity for high pressure in the network. For example, if during the hours when the water pressure is usually low (noon), a possibility of power generation occurs, then the method is able to detect it and activate the PAT, as shown in the tables in Section 9. Of course, the current methodology does not analyze the further operation of the PATs and the problems that arise due to the change in flow. This could be the subject of an extension of the present study. To find the “window” of PAT activation, the harmony search algorithm was used, which decides when the PAT can be activated and how much energy we can remove from the node without the collapse of the rest of the network. The algorithm decides which times and how much pressure can theoretically be recovered from the nodes in 24 h, while ensuring the smooth operation of the rest of the network. According to the optimization model, the maximum possible pressure per time step can be recovered without a pressure lack at the other nodes. In this way, the real-time operation of the system is possible. According to the results tables, which concern a benchmark network, there are time steps (hours) available for energy recovery. The performance of PATs and how they take advantage of hourly stress opportunities could also be an extension of the present study.

Author Contributions: Conceptualization, D.K. and N.T.; methodology, D.K. and N.T.; software, D.K. and N.T.; validation, D.K. and N.T.; resources, D.K. and N.T.; data curation, D.K. and N.T.; writing—review and editing, D.K. and N.T.; visualization, D.K. and N.T.; supervision, N.T. All authors have read and agreed to the published version of the manuscript.

Funding: This research received no external funding.

Institutional Review Board Statement: Not applicable.

Informed Consent Statement: Not applicable.

Data Availability Statement: Not applicable.

Conflicts of Interest: The authors declare no conflict of interest.

Abbreviations

WDN	Water Distribution Network
PRV	Pressure Reducing Valve
PATs	Pumps As Turbines
WSN	Wireless Sensor Network
WNTR	Water Network Tool for Resilience
ANN	Artificial Neural Network
ML	Machine Learning
ReLU	Rectified Linear Unit
BPT	Break Pressure Tank
PBV	Pressure Breaker Valve
HM	Harmony Memory
HSA	Harmony Search Algorithm
HMCR	Harmony Memory Consideration Ratio
HMS	Harmony Memory Size
PAR	Pitch Adjustment Rate
BET	Best Efficiency Point
MHP	Micro Hydro Power
CFD	Computational Fluid Dynamics

References

1. Gonçalves, F.V.; Costa, L.H.; Ramos, H.M. ANN for Hybrid Energy System Evaluation: Methodology and WSS Case Study. *Water Resour. Manag.* **2011**, *25*, 2295–2317. [CrossRef]
2. Vicente, D.J.; Garrote, L.; Sanchez, R.; Santillan, D. Pressure management in water distribution systems: Current status, proposals, and future trends. *J. Water Resour. Plan. Manag.* **2015**, *142*, 04015061. [CrossRef]
3. Nazif, S.; Karamouz, M.; Tabesh, M.; Moridi, A. Pressure Management Model for Urban Water Distribution Net-works. *Water Resour. Manag.* **2010**, *24*, 437–458. [CrossRef]
4. Araujo, L.; Ramos, H.; Coelho, S. Pressure control for leakage minimization in water distribution systems man-agement. *Water Resour. Manag.* **2006**, *20*, 133–149. [CrossRef]
5. Vairavamoorthy, K.; Lumbers, J. Leakage Reduction in Water Distribution Systems: Optimal Valve Control. *J. Hydraul. Eng.* **1998**, *124*, 1146–1154. [CrossRef]
6. Prescott, S.L.; Ulanicki, B. Improved Control of Pressure Reducing Valves in Water Distribution Networks. *J. Hydraul. Eng.* **2008**, *134*, 56–65. [CrossRef]
7. Almandoz, J.; Cabrera, E.; Arregui, F.; Cobacho, R. Leakage Assessment through Water Distribution Network Simulation. *J. Water Resour. Plan. Manag.* **2005**, *131*, 458–466. [CrossRef]
8. Walsky, T.; Bezts, W.; Posluzny, E.; Weir, M.; Withman, B. Modeling leakage reduction through pressure control. *J. Am. Water Works Ass.* **2006**, *98*, 148–155. [CrossRef]
9. De Paola, F.; Giugni, M.; Portolano, D. Pressure Management Through Optimal Location and Set-ting of Valves in Water Distribution Networks Using a Music-Inspired Approac. *Water Resour. Manag.* **2017**, *31*, 1517–1533. [CrossRef]
10. De Paola, F.; Fontana, N.; Galdiero, E.; Giugni, M.; Savic, D.A.; Sorgenti degli Uberti, G. Automatic multiobjective sectori-zation of a water distribution network. *Procedia Eng.* **2014**, *89*, 1200–1207. [CrossRef]
11. De Paola, F.; Galdiero, E.; Giugni, M. A jazz-based approach for optimal setting of pressure reducing valves in water distribution networks. *Eng. Optim.* **2015**, *48*, 727–739. [CrossRef]
12. Liberatore, S.; Sechi, G.M. Location and calibration of valves in water distribution networks using a scatter-search meta-heuristic approach. *Water Resour. Manag.* **2009**, *23*, 1479–1495. [CrossRef]

13. Page, P.R.; Abu-Mahfouz, A.M.; Mothetha, M.L. Pressure Management of Water Distribution Systems via the Remote Real-Time Control of Variable Speed Pumps. *J. Water Resour. Plan. Manag.* **2017**, *143*, 1–11. [CrossRef]
14. Page, P.R.; Abu-Mahfouz, A.M.; Yoyo, S. Real-time adjustment of pressure to demand in water distribution systems: Parameter-less P-controller algorithm. In Proceedings of the 12th International Conference on Hydroinformatics, HIC, Incheon, Korea, 21–26 August 2016.
15. Carravetta, A.; Fecarotta, O.; Del Gidice, G.; Ramos, H. Energy recovery in water systems by PATs: A comparisons among the different installation schemes. *Procedia Eng.* **2014**, *70*, 275–284. [CrossRef]
16. Carravetta, A.; Fecarotta, O.; Martino, R.; Antipodi, L. PAT efficiency variation with design parameters. *Procedia Eng.* **2014**, *70*, 285. [CrossRef]
17. Filion, Y.; MacLean, H.; Karney, B. Life Cycle Energy Analysis of a Water Distribution System. *J. Infrastruct. Syst.* **2014**, *10*, 120–130. [CrossRef]
18. Sammartano, V.; Aricò, C.; Carravetta, A.; Fecarotta, O.; Tucciarelli, T. Banki-michell optimal design by computational fluid dynamics testing and hydrodynamic analysis. *Energies* **2013**, *6*, 2362–2385. [CrossRef]
19. Paish, O. Small hydro power: Technology and current status. *Renew. Sustain. Energy Rev.* **2002**, *6*, 537–556. [CrossRef]
20. Ramos, H.M.; Mello, M.; De, P.K. Clean power in water supply systems as a sustainable solution: From planning to practical implementation. *Water Sci. Technol. Water Supply* **2010**, *10*, 39–49. [CrossRef]
21. Lugauer, F.J.; Kainz, J.; Gaderer, M. Techno-Economic Efficiency Analysis of Various Operating Strategies for Micro-Hydro Storage Using a Pump as a Turbine. *Energies* **2021**, *14*, 425. [CrossRef]
22. Lugauer, F.J.; Kainz, J.; Gehlich, E.; Gaderer, M. Roadmap to Profitability for a Speed-Controlled Micro-Hydro Storage System Using Pumps as Turbines. *Sustainability* **2022**, *14*, 653. [CrossRef]
23. Stefanizzi, M.; Capurso, T.; Balacco, G.; Binetti, M.; Camporeale, S.M.; Torresi, M. Selection, control and techno-economic feasibility of Pumps as Turbines in Water Distribution Networks. *Renew. Energy* **2020**, *162*, 1292–1306. [CrossRef]
24. Stefanizzi, M.; Capurso, T.; Balacco, G.; Binetti, M.; Torresi, M.; Camporeale, S.M. Pump as turbine for throttling energy recovery in water distribution networks. *AIP Conf. Proc.* **2019**, *2191*, 020142. [CrossRef]
25. Kramer, M.; Terheiden, K.; Wieprecht, S. Pumps as turbines for efficient energy recovery in water supply networks. *Renew. Energy* **2018**, *122*, 17–25. [CrossRef]
26. Novara, D.; Carravetta, A.; McNabola, A.; Ramos, H.M. Cost Model for Pumps as Turbines in Run-of-River and In-Pipe Microhydropower Applications. *J. Water Resour. Plan. Manag.* **2019**, *145*, 04019012. [CrossRef]
27. Chacón, M.C.; Díaz, J.A.R.; Morillo, J.G.; McNabola, A. Hydropower energy recovery in irrigation networks: Validation of a methodology for flow prediction and pump as turbine selection. *Renew. Energy* **2019**, *147*, 1728–1738. [CrossRef]
28. García, I.F.; Novara, D.; Mc Nabola, A. A Model for Selecting the Most Cost-Effective Pressure Control Device for More Sustainable Water Supply Networks. *Water* **2019**, *11*, 1297. [CrossRef]
29. Knapp, R.T. Complete characteristics of centrifugal pumps and their use in the prediction of transient behaviour. *Trans. ASME* **1937**, *59*, 683–689.
30. Balacco, G. Performance Prediction of a Pump as Turbine: Sensitivity Analysis Based on Artificial Neural Networks and Evolutionary Polynomial Regression. *Energies* **2018**, *11*, 3497. [CrossRef]
31. Rossi, M.; Renzi, M. A general methodology for performance prediction of pumps-as-turbines using Artificial Neural Networks. *Renew. Energy* **2018**, *128*, 265–274. [CrossRef]
32. Liu, M.; Tan, L.; Cao, S. Theoretical model of energy performance prediction and BEP determination for centrifugal pump as turbine. *Energy* **2019**, *172*, 712–732. [CrossRef]
33. Venturini, M.; Alvisi, S.; Simani, S.; Manservigi, L. Comparison of Different Approaches to Predict the Performance of Pumps as Turbines (PATs). *Energies* **2018**, *11*, 1016. [CrossRef]
34. Venturini, M.; Manservigi, L.; Alvisi, S.; Simani, S. Development of a physics-based model to predict the performance of pumps as turbines. *Appl. Energy* **2018**, *231*, 343–354. [CrossRef]
35. Morabito, A.; Hendrick, P. Pump as turbine applied to micro energy storage and smart water grids: A case study. *Appl. Energy* **2019**, *241*, 567–579. [CrossRef]
36. Barbarelli, S.; Amelio, M.; Florio, G. Experimental activity at test rig validating correlations to select pumps running as turbines in microhydro plants. *Energy Convers. Manag.* **2017**, *149*, 781–797. [CrossRef]
37. Hamlehdar, M.; Yousefi, H.; Noorollahi, Y.; Mohammadi, M. Energy recovery from water distribution networks using micro hydropower: A case study in Iran. *Energy* **2022**, *252*, 124024. [CrossRef]
38. Da Silva, B.L.A.; Lafay, J.-M.S.; Tofoli, F.L.; Scartazzini, L.S. Case Study: Hydroelectric Generation Employing the Water Distribution Network in Pato Branco, Brazil. *Proc. IASTED Int. Conf. Power Energy Syst. Eur.* **2011**, *2011*, 50–54. [CrossRef]
39. Giugni, M.; Fontana, N.; Portolano, D. Energy saving policy in water distribution networks. *Renew. Energy Power Qual. J.* **2009**, *1*, 733–738. [CrossRef]
40. Corcoran, L.; McNabola, A.; Coughlan, P. Energy recovery potential of the Dublin region water supply network. In *Water Congress on Water*; Climate and Energy: Dublin, Ireland, 2012.
41. Möderl, M.; Sitzenfrei, R.; Mair, M.; Jarosch, H.; Rauch, W. Identifying Hydropower Potential in Water Distribution Systems of Alpine Regions. In *World Environmental and Water Resources Congress 2012: Crossing Boundaries*; ASCE: Reston, VA, USA, 2012.

42. Balacco, G.; Binetti, M.; Capurso, T.; Stefanizzi, M.; Torresi, M.; Piccinni, A.F. Pump as Turbine for the Energy Recovery in a Water Distribution Network: Two Italian (Apulian) Case Studies. *Environ. Sci. Proc.* **2020**, *2*, 1. [CrossRef]
43. Zaman, D.; Tiwari, M.K.; Gupta, A.K.; Sen, D. Performance indicators-based energy sustainability in urban water distribution networks: A state-of-art review and conceptual framework. *Sustain. Cities Soc.* **2021**, *72*, 103036. [CrossRef]
44. Ávila, C.A.M.; Sánchez-Romero, F.-J.; López-Jiménez, P.A.; Pérez-Sánchez, M. Optimization tool to improve the management of the leakages and recovered energy in irrigation water systems. *Agric. Water Manag.* **2021**, *258*, 107223. [CrossRef]
45. Giudicianni, C.; Herrera, M.; di Nardo, A.; Carravetta, A.; Ramos, H.M.; Adeyeye, K. Zero-net energy management for the monitoring and control of dynamically-partitioned smart water systems. *J. Clean. Prod.* **2019**, *252*, 119745. [CrossRef]
46. Fontana, N.; Giugni, M.; Glielmo, L.; Marini, G.; Zollo, R. Hydraulic and Electric Regulation of a Prototype for Real-Time Control of Pressure and Hydropower Generation in a Water Distribution Network. *J. Water Resour. Plan. Manag.* **2018**, *144*, 4018072. [CrossRef]
47. Creaco, E.; Galuppini, G.; Campisano, A.; Ciaponi, C.; Pezzinga, G. A Bi-Objective Approach for Optimizing the Installation of PATs in Systems of Transmission Mains. *Water* **2020**, *12*, 330. [CrossRef]
48. García, A.M.; Gallagher, J.; Chacón, M.C.; Mc Nabola, A. The environmental and economic benefits of a hybrid hydropower energy recovery and solar energy system (PAT-PV), under varying energy demands in the agricultural sector. *J. Clean. Prod.* **2021**, *303*, 127078. [CrossRef]
49. Mousavi, N.; Kothapalli, G.; Habibi, D.; Lachowicz, S.W.; Moghaddam, V. A real-time energy management strategy for pumped hydro storage systems in farmhouses. *J. Energy Storage* **2020**, *32*, 101928. [CrossRef]
50. Jowitt, P.W.; Xu, C. Optimal valve control in water-distribution networks. *J. Water Res. Pl-ASCE* **1990**, *116*, 455–472. [CrossRef]
51. Dai, P.D.; Li, P. Optimal Pressure Regulation in Water Distribution Systems Based on an Extended Model for Pressure Reducing Valves. *Water Resour. Manag.* **2016**, *30*, 1239–1254. [CrossRef]
52. Cao, H.; Hopfgarten, S.; Ostfeld, A.; Salomons, E.; Li, P. Simultaneous Sensor Placement and Pressure Reducing Valve Localization for Pressure Control of Water Distribution Systems. *Water* **2019**, *11*, 1352. [CrossRef]
53. Sterling, M.; Bargiela, A. Leakage reduction by optimised control of valves in water networks. *Trans. Inst. Meas. Control* **1984**, *6*, 293–298. [CrossRef]
54. Nguyen, K.D.; Dai, P.D.; Vu, D.Q.; Cuong, B.M.; Tuyen, V.P.; Li, P. A MINLP Model for Optimal Localization of Pumps as Turbines in Water Distribution Systems Considering Power Generation Constraints. *Water* **2020**, *12*, 1979. [CrossRef]
55. WSAA. *Water Supply Code of Australia, Melbourne Retail Water Agencies*; WSAA: Melbourne, Australia, 2002.
56. Trifunovic, N. *Introduction to Urban Water Distribution: Unesco-IHE Lecture Note Series*, 1st ed.; CRC Press: Boca Raton, FL, USA, 2006. [CrossRef]
57. Smith, M.A.; Shneiderman, B.; Milic-Frayling, N.; Mendes Rodrigues, E.; Barash, V.; Dunne, C.; Capone, T.; Perer, A.; Gleave, E. *Analyzing Social Media Networks with NodeXL*, 2nd ed.; Morgan Kaufmann: Burlington, MA, USA, 2020.
58. Hagberg, A.; Swart, P.; Chult, D.S. Exploring network structure, dynamics, and function using NetworkX. In Proceedings of the 7th Python in Science Conference (SciPy2008), Pasadena, CA, USA, 21 August 2008; pp. 11–15.
59. Klise, K.A.; Hart, D.; Moriarty, D.M.; Bynum, M.L.; Murray, R.; Burkhardt, J.; Haxton, T. *Water Network Tool for Resilience (WNTR) User Manual*; U.S. Environmental Protection Agency Technical Report, EPA/600/R-17/264; Sandia National Lab.: Albuquerque, NM, USA, 2017; 47p. [CrossRef]
60. Kucukali, S. Municipal water supply dams as a source of small hydropower in Turkey. *Renew. Energy* **2010**, *35*, 2001–2007. [CrossRef]
61. Kougias, I.; Patsialis, T.; Zafirakou, A.; Theodossiou, N. Exploring the potential of energy recovery using micro hydropower systems in water supply systems. *Water Util. J.* **2014**, *7*, 25–33.
62. Rossi, M.; Nigro, A.; Renzi, M. Experimental and numerical assessment of a methodology for performance prediction of Pumps-as-Turbines (PaTs) operating in off-design conditions. *Appl. Energy* **2019**, *248*, 555–566. [CrossRef]
63. Yang, S.-S.; Derakhshan, S.; Kong, F.-Y. Theoretical, numerical and experimental prediction of pump as turbine performance. *Renew. Energy* **2012**, *48*, 507–513. [CrossRef]
64. Williams, A. The turbine performance of centrifugal pumps: A Comparison of prediction methods. *J. Power Energy* **1994**, *208*, 59–66. [CrossRef]
65. Krivchenko, G. *Hydraulic Machines: Turbines and Pumps*; Lewis: Boca Raton, FL, USA, 1994.
66. Wang, T.; Kong, F.; Yang, S.; Fu, Y. Numerical Study on Hydraulic Performances of Pump as Turbine with Forward-Curved Blades. In Proceedings of the Fluids Engineering Division Summer Meeting. American Society of Mechanical Engineers, Chicago, IL, USA, 3–7 August 2014.
67. Plua, F.; Hidalgo, V.; López-Jiménez, P.; Pérez-Sánchez, M. Analysis of Applicability of CFD Numerical Studies Applied to Problem When Pump Working as Turbine. *Water* **2021**, *13*, 2134. [CrossRef]
68. Yang, W.; Xiao, R. Multiobjective Optimization Design of a Pump–Turbine Impeller Based on an Inverse Design Using a Combination Optimization Strategy. *J. Fluids Eng.* **2013**, *136*, 014501. [CrossRef]
69. Zhu, B.; Wang, X.; Tan, L.; Zhou, D.; Zhao, Y.; Cao, S. Optimization design of a reversible pump–turbine runner with high efficiency and stability. *Renew. Energy* **2015**, *81*, 366–376. [CrossRef]
70. Capurso, T.; Stefanizzi, M.; Pascazio, G.; Camporeale, S.M.; Torresi, M. Dependency of the slip phenomenon on the inertial forces inside radial runners. *AIP Conf. Proc.* **2019**, *2191*, 020034. [CrossRef]

71. Jain, S.V.; Patel, R. Investigations on pump running in turbine mode: A review of the state-of-the-art. *Renew. Sustain. Energy Rev.* **2014**, *30*, 841–868. [CrossRef]
72. Woo, Z.; Hoon, J.; Loganathan, G.V. A New Heuristic Optimization Algorithm: Harmony Search. *Simulation* **2001**, *76*, 60–68.
73. Bermúdez, J.; López-Estrada, F.; Besançon, G.; Torres, L.; Santos-Ruiz, I. Leak-Diagnosis Approach for Water Distribution Networks based on a k-NN Classification Algorithm. *IFAC-PapersOnLine* **2020**, *53*, 16651–16656. [CrossRef]